TAMPERE UNIVERSITY OF TECHNOLOGY

Author(s) Chen, Liang.; Ali-Löytty, Simo; Piché, Robert; Wu, Lenan

Title Mobile tracking in mixed line-of-sight/non-line-of-sight conditions: Algorithm and theoretical lower bound

Citation Chen, Liang.; Ali-Löytty, Simo; Piché, Robert; Wu, Lenan 2012. Mobile tracking in mixed line-of-sight/non-line-of-sight conditions: Algorithm and theoretical lower bound. Wireless Personal Communications vol. 65, num. 4, 753-771.

Year 2012

DOI http://dx.doi.org/10.1007/s11277-011-0294-7

Version Post-print

URN http://URN.fi/URN:NBN:fi:tty-201311061421

Copyright The final publication is available at link.springer.com.

All material supplied via TUT DPub is protected by copyright and other intellectual property rights, and duplication or sale of all or part of any of the repository collections is not permitted, except that material may be duplicated by you for your research use or educational purposes in electronic or print form. You must obtain permission for any other use. Electronic or print copies may not be offered, whether for sale or otherwise to anyone who is not an authorized user.

Mobile Tracking in Mixed Line-of-sight/Non-line-of-sight Conditions: Algorithm and Theoretical Lower Bound

Chen Liang · Simo Ali-Löytty · Robert Piché · Wu Lenan

Abstract The paper investigates the problem of mobile tracking in mixed line-of-sight (LOS)/non-line-of-sight (NLOS) conditions. The motion of mobile station is modeled by a dynamic white noise acceleration model, while the measurements are Time of Arrival (TOA). A first-order Markov model is employed to describe the dynamic transition of LOS/NLOS conditions. An improved Rao-Blackwellized particle filter (RBPF) is proposed, in which the LOS/NLOS sight conditions are estimated by particle filtering using the optimal trial distribution, and the mobile state is computed by applying approximated analytical methods. The theoretical error lower bound is further studied in the described problem. A new method is presented to compute the posterior Cramer-Rao lower bound (CRLB): the mobile state is first estimated by decentralized extended Kalman filter (EKF) method, then sigma point set and unscented transformation are applied to calculate Fisher information matrix (FIM). Simulation results show that the improved RBPF is more accurate than current methods, and its performance approaches to the theoretical bound.

Chen Liang
Mathematics Department, Tampere University of Technology, Finland
Tel.: +358-40-198-1991
Fax: +358-3-3115-3549
E-mail: liang.chen@tut.fi
Present address: Korkeakoulunkatu 1, P.O. Box 533, 33101 Tampere, Finland

Simo Ali-Löytty
Mathematics Department, Tampere University of Technology, Finland
E-mail: simo.ali-loytty@tut.fi

Robert Piché
Mathematics Department, Tampere University of Technology, Finland
E-mail: robert.piche@tut.fi

Wu Lenan
School of Information Science and Technology, Southeast University, Nanjing, China
E-mail: wuln@seu.edu.cn

Keywords mobile tracking · non-line-of-sight (NLOS) · extended Kalman filter (EKF) · Rao-Blackwellization · particle filtering · Cramer-Rao lower bound (CRLB)

1 Introduction

Mobile positioning using radio signals has received considerable attentions over the past decades. Different kinds of location systems have been developed for various kinds of applications, such as satellite positioning systems like global positioning system (GPS) and GALILEO, cellular based positioning systems, and indoor positioning system based on ultrawideband (UWB) signals.

However, precise positioning in non-line-of-sight (NLOS) conditions is still a tough task. In NLOS conditions, the direct path between the transmitter and receiver has been blocked by buildings and other obstacles. Propagation wave may actually travel excess path lengths due to effects of reflection, refraction and scattering. In terms of range based measurements such as time of arrival (TOA), time difference of arrival (TDOA) and receiver signal strength (RSS), this extra propagation distance imposes positive biases on the true path, which cause large errors on the location estimations. In dense urban regions, the non-line-of-sight (NLOS) condition is very common. For example, a field test in GSM network shows that the mean and standard deviation of NLOS range errors are on the order of 513 m and 436 m respectively [1].

Several methods have been proposed to deal with the NLOS problem. Generally, these methods can be divided into two categories: methods for static positioning systems and methods for mobility tracking systems. The methods for static positioning systems can be further divided into three ways. The first way is to detect and identify the LOS signals for localization [2–5]. The second way is to mitigate the NLOS effect and minimize the estimate error, which include weights or scaling factors [6, 7], and equalization method [8]. The third way is to model the NLOS propagation paths. Scattering models [9, 10], multipath information in the time domain [11] or space-time domain [12] are employed to achieve this kind of objective.

In mobility tracking systems, the general idea is to exploit the redundant measurements in time series to mitigate the NLOS errors. Assuming that the standard deviation of the range measurement in the case of NLOS is significantly larger than that of LOS, polynomial fit [13] and two-step Kalman filtering techniques [14] are applied to smooth range measurements and mitigate NLOS errors. However, the problem is that the deviation threshold needs to be carefully considered to decrease the false detection of LOS signals. A Markov process is introduced to describe the LOS and NLOS condition as two interactive modes in [15]. A Kalman based interacting multiple model (IMM) smoother is further proposed to estimate the range between the corresponding base station (BS) and mobile station (MS). It can track the true range distance more accurately than the rough LOS/NLOS smoother in [14], especially in the transitional intervals. The method in [16] uses a first-order

homogeneous hidden Markov chain to simultaneously model the transition of LOS/NLOS condition and receiver position. Grid based Bayesian estimation [16] and particle filtering [17] are used for UWB indoor positioning. In our previous work in [18], a modified extended Kalman filter (EKF) is proposed to jointly estimate the mobile state and the LOS/NLOS sight state based on the measurements from single BS. Then Bayesian data fusion algorithm is further applied to improve the estimation accuracy. Simulation results show the performance improvement over the method in [14, 15], and that the location errors of the method are all significantly smaller than that of the Federal Communication Commission (FCC) requirement [19] in different LOS/NLOS conditions.

In this paper, we continue to investigate the mobile tracking problem in mixed LOS/NLOS conditions. An improved Rao-Blackwellized particle filtering (RBPF) method is proposed for mobility tracking. The method firstly estimates the sight condition state using particle filtering, then applies decentralized EKF method to analytically compute the mobile state. Meanwhile, a theoretical lower bound of the described problem is also derived under the assumption that the LOS and NLOS transition history is known, which avoids the false detection of sight condition. A new method is presented to calculate the posterior CRLB, which adopts the decentralized EKF method to estimate the mobile state first, then applies sigma point set and unscented transformation to calculate Fisher information matrix (FIM), the inverse of posterior Cramer-Rao lower bound (CRLB) value. The posterior CRLB we derive could be used as the theoretical basis for evaluating new positioning algorithms. It is also useful in predicting the performance for various sampling intervals and sensor accuracy. Although we study the theoretical lower bound in the context of mobile cellular positioning, the methodology is completely general for other platforms, such as UWB, satellite based position etc.

The paper is organized as follows: Section 2 presents the dynamic system models and formulates the problem of mobility tracking in the mixed LOS/NLOS conditions. The proposed RBPF method is presented in Section 3. Section 4 describes the derivation of the performance lower bound. Numerical results and performance comparison are presented and discussed in Section 5. Section 6 draws some conclusions.

2 System Description

2.1 State Model

In this work, we assume a mobile of interest moves on a two-dimensional Cartesian plane, and the state at time instant t_k is defined as the vector

$$\mathbf{x}_k = \left[x_k \; y_k \; \dot{x}_k \; \dot{y}_k \right]^T,$$

where $\left[x_k \; y_k \right]^T$ corresponds to the east and north coordinates of the mobile position; $\left[\dot{x}_k \; \dot{y}_k \right]^T$ are the corresponding velocities. The mobile state with

random acceleration can be modeled as [20, p. 267]:

$$\mathbf{x}_{k+1} = \Phi_k \mathbf{x}_k + \mathbf{w}_k, \tag{1}$$

where the state transition matrix $\Phi_k = \begin{bmatrix} \mathrm{I}_2 & \Delta t_k \mathrm{I}_2 \\ 0 & \mathrm{I}_2 \end{bmatrix}$, with I_2 the 2×2 matrix and $\Delta t_k = t_{k+1} - t_k$. The random process $\mathbf{w}_k$ is a white zero mean Gaussian noise, with covariance matrix

$$\mathrm{Q}_k = \begin{bmatrix} \frac{\Delta t_k^4}{4}\mathrm{Q} & \frac{\Delta t_k^3}{2}\mathrm{Q} \\ \frac{\Delta t_k^3}{2}\mathrm{Q} & \Delta t_k^2 \mathrm{Q} \end{bmatrix},$$

where $\mathrm{Q} = \begin{bmatrix} \sigma_x^2 & 0 \\ 0 & \sigma_y^2 \end{bmatrix}$.

2.2 Measurement Model

In existing cellular systems, the range can be measured by TOA method. Suppose $d_{i,k}$ represents the true distance between the mobile position $\begin{bmatrix} x_k & y_k \end{bmatrix}^T$ and the location of the ith BS $\begin{bmatrix} x_{\mathrm{bs}_i} & y_{\mathrm{bs}_i} \end{bmatrix}^T$:

$$d_{i,k} \triangleq h_{i,k}(\mathbf{x}_k) = \sqrt{(x_k - x_{\mathrm{bs}_i})^2 + (y_k - y_{\mathrm{bs}_i})^2}, \tag{2}$$

where $i \in \{1, 2, \ldots, M\}$ and M is the number of base stations. In a LOS environment, the range measurement between MS and BS_i is only corrupted by the system measurement noise $n_{i,k}$, which can be modeled as an independent and identically distributed (i.i.d.) zero mean white Gaussian noise $\mathrm{N}(0, \sigma_n^2)$. In NLOS conditions, the range measurement is corrupted by two sources of errors: the measurement noise $n_{i,k}$ and the NLOS error $e_{i,k}$. According to the field tests in [1], $e_{i,k}$ can be modeled as a positively biased distribution. In this paper we assume that NLOS error have Gaussian distribution $\mathrm{N}(\mu_{\mathrm{NLOS}}, \sigma_{\mathrm{NLOS}}^2)$, the same assumptions as is used in publications [14, 15, 18, 21, 22]. We also assume that errors $n_{i,k}$ and $e_{i,k}$ are independent. Then the range measurement equations are

$$\text{LOS}: \qquad z_{i,k} = d_{i,k} + n_{i,k} \tag{3a}$$

$$\text{NLOS}: \qquad z_{i,k} = d_{i,k} + n_{i,k} + e_{i,k}. \tag{3b}$$

We introduce a Boolean variable $s_{i,k} \in \{0, 1\}$ to represent LOS/NLOS condition between the MS and BS_i at time instant k, with $s_{i,k} = 0$ for LOS and $s_{i,k} = 1$ for NLOS. Equations (3a) and (3b) can then be written as

$$z_{i,k} = d_{i,k} + v(s_{i,k}), \tag{4}$$

where, $v(s_{i,k}) \sim \mathrm{N}(m(s_{i,k}), \mathrm{R}(s_{i,k}))$ and

$$m(s_{i,k}) = s_{i,k}\mu_{\mathrm{NLOS}} \tag{5a}$$

$$\mathrm{R}(s_{i,k}) = \sigma_n^2 + s_{i,k}\sigma_{\mathrm{NLOS}}^2. \tag{5b}$$

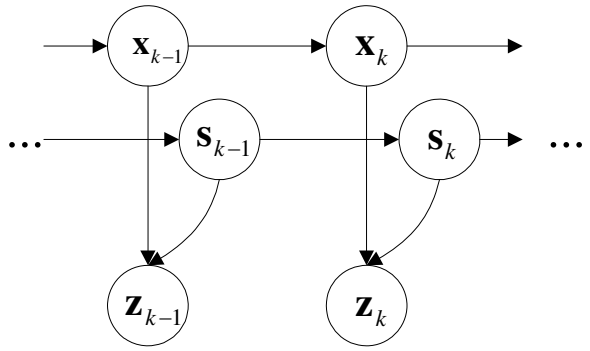

Fig. 1 Overall mobility tracking model

Field measurements have shown a dynamic transition between LOS and NLOS conditions in typical cellular communication environments [23]. Thus, the transitions of the two-state sight condition variable $s_{i,k}$ can be further assumed as a time-homogeneous first-order Markov chain $s_{i,k} \sim \mathrm{MC}(\pi_i, \mathrm{A}_i)$ with initial probability vector π_i and transition probability matrix

$$\mathrm{A}_i = \begin{bmatrix} \mathrm{P}(s_{i,k}=0|s_{i,k-1}=0)\ \mathrm{P}(s_{i,k}=1|s_{i,k-1}=0) \\ \mathrm{P}(s_{i,k}=0|s_{i,k-1}=1)\ \mathrm{P}(s_{i,k}=1|s_{i,k-1}=1) \end{bmatrix}. \tag{6}$$

We assume that the transition probability matrix A_i is constant. Denoting $\mathrm{P}(s_{i,k}=0|s_{i,k-1}=0)=p_0$ and $\mathrm{P}(s_{i,k}=1|s_{i,k-1}=1)=p_1$, the transition probability matrix can be written as

$$\mathrm{A}_i = \begin{bmatrix} p_0 & 1-p_0 \\ 1-p_1 & p_1 \end{bmatrix}, \text{for all}\, i.$$

Note that the sight condition of each BS is governed by its own independent Markov chain.

2.3 Problem Formulation

To sum up, the overall dynamic model of the mobility tracking in the mixed LOS/NLOS conditions can be represented as follows:

$$\begin{cases} \mathbf{x}_k = \Phi_{k-1}\mathbf{x}_{k-1} + \mathbf{w}_{k-1} \\ s_{i,k} \sim \mathrm{MC}(\pi_i, \mathrm{A}_i) \\ \mathbf{z}_k = \mathbf{h}_k(\mathbf{x}_k) + \mathbf{v}_k(\mathbf{s}_k) \end{cases}, \tag{7}$$

where $s_{i,k}$ is the ith component of vector $\mathbf{s}_k$, $i \in \{1, 2, \ldots, M\}$, $k \in \mathbb{N}$. To facilitate the understanding, the model is further depicted in Fig. 1.

Denote the total observation sequence up to time t_k as $\mathbf{z}_{1:k}$, where $\mathbf{z}_k \triangleq [z_{1,k}, z_{2,k}, \ldots, z_{M,k}]^T$ The problem of mobile tracking in mixed LOS/NLOS conditions is to infer the current mobile state $\mathbf{x}_k$ from the observation $\mathbf{z}_{1:k}$,

that is, to compute the marginal posterior $p(\mathbf{x}_k|\mathbf{z}_{1:k})$. The marginal posterior is the mixture

$$p(\mathbf{x}_k|\mathbf{z}_{1:k}) = \sum_{\mathrm{s}_k} p(\mathbf{x}_k, \mathbf{s}_k = \mathrm{s}_k|\mathbf{z}_{1:k}), \tag{8}$$

where s_k go through all 2^M possibilities. Components of mixture (which are also mixtures) $p(\mathbf{x}_k, \mathbf{s}_k = \mathrm{s}_k|\mathbf{z}_{1:k})$ can be determined recursively according to the following relations [24, Ch. 1].
Prediction:

$$\begin{aligned} p(\mathbf{x}_k, \mathbf{s}_k = \mathrm{s}_k|\mathbf{z}_{1:k-1}) = \sum_{\mathrm{s}_{k-1}} \Bigg(\mathrm{P}(\mathbf{s}_k = \mathrm{s}_k|\mathbf{s}_{k-1} = \mathrm{s}_{k-1}) \times \\ \int p(\mathbf{x}_k|\mathbf{x}_{k-1}) p(\mathbf{x}_{k-1}, \mathbf{s}_{k-1} = \mathrm{s}_{k-1}|\mathbf{z}_{1:k-1}) \mathrm{d}\mathbf{x}_{k-1} \Bigg); \end{aligned} \tag{9}$$

Update:

$$p(\mathbf{x}_k, \mathbf{s}_k = \mathrm{s}_k|\mathbf{z}_{1:k}) = \frac{p(\mathbf{z}_k|\mathbf{x}_k, \mathbf{s}_k = \mathrm{s}_k) p(\mathbf{x}_k, \mathbf{s}_k = \mathrm{s}_k|\mathbf{z}_{1:k-1})}{\sum_{\mathrm{s}_k} \int p(\mathbf{z}_k|\mathbf{x}_k, \mathbf{s}_k = \mathrm{s}_k) p(\mathbf{x}_k, \mathbf{s}_k = \mathrm{s}_k|\mathbf{z}_{1:k-1}) \mathrm{d}\mathbf{x}_k}, \tag{10}$$

where the transition probability is

$$\mathrm{P}(\mathbf{s}_k = \mathrm{s}_k|\mathbf{s}_{k-1} = \mathrm{s}_{k-1}) = \prod_{i=1}^{M} \mathrm{P}(s_{i,k} = \mathrm{s}_{i,k}|s_{i,k-1} = \mathrm{s}_{i,k-1}), \tag{11}$$

the transitional density is

$$p(\mathbf{x}_k|\mathbf{x}_{k-1}) = p_{\mathbf{w}_{k-1}}(\mathbf{x}_k - \Phi_{k-1}\mathbf{x}_{k-1})$$

and the likelihood is

$$p(\mathbf{z}_k|\mathbf{x}_k, \mathbf{s}_k = \mathrm{s}_k) = p_{\mathbf{v}_k(\mathbf{s}_k = \mathrm{s}_k)}(\mathbf{z}_k - \mathbf{h}_k(\mathbf{x}_k)).$$

The solution to (10) cannot be derived analytically, because measurement function $\mathbf{h}$ is nonlinear. Moreover the number of mixture components grows exponentially with time. For this reason, several suboptimal solutions have been proposed, in which different approximation methods have been applied [14, 15, 18]. The sequential Monte-Carlo (SMC) method (also called particle filtering) has proven to be successful in tracking applications with nonlinear and non-Gaussian models [24]. Here, we resort to this kind of sample-based numerical approximate method to solve the inference problem of this work.

3 New tracking algorithm based on improved RBPF

The basic idea behind particle filters is as follows. Denote $\mathbf{y}_k \triangleq \begin{bmatrix} \mathbf{x}_k \\ \mathbf{s}_k \end{bmatrix}$, and suppose a set of N weighted samples $\{\mathbf{y}_{k-1}^{(j)}, w_{k-1}^{(j)}\}_{j=1}^{N}$ is used to approximate the posterior $p(\mathbf{y}_{k-1}|\mathbf{z}_{1:k-1})$ at time t_{k-1} with the following point-distribution

$$p(\mathbf{y}_{k-1}|\mathbf{z}_{1:k-1}) \approx \sum_{j=1}^{N} w_{k-1}^{(j)} \delta(\mathbf{y}_{k-1} - \mathbf{y}_{k-1}^{(j)}), \tag{12}$$

where $\delta(\cdot)$ denotes the Dirac-delta function.

Then, new samples $\mathbf{y}_k^{(j)}$ are generated from a suitably designed proposal distribution $q(\mathbf{y}_k|\mathbf{y}_{k-1}^{(j)}, \mathbf{z}_k)$, which may depend on the old state and the new measurement. The new importance weights are set to

$$w_k^{(j)} \propto w_{k-1}^{(j)} \frac{p(\mathbf{z}_k|\mathbf{y}_k^{(j)}) p(\mathbf{y}_k^{(j)}|\mathbf{y}_{k-1}^{(j)})}{q(\mathbf{y}_k^{(j)}|\mathbf{y}_{k-1}^{(j)}, \mathbf{z}_k)}. \tag{13}$$

Thus, a new set of samples $\{\mathbf{y}_k^{(j)}, w_k^{(j)}\}_{j=1}^{N}$ is approximately distributed according to $p(\mathbf{y}_k|\mathbf{z}_{1:k})$ at time t_k by the above SMC procedure.

Since, in most cases, it is difficult or computationally too expensive to directly sample from the posterior, some trial sample densities can be used to draw particles. In standard particle filtering, transition priors are utilized as the proposal distribution

$$q(\mathbf{y}_k|\mathbf{y}_{k-1}^{(j)}, \mathbf{z}_k) = p(\mathbf{y}_k|\mathbf{y}_{k-1}^{(j)}) = p(\mathbf{x}_k|\mathbf{x}_{k-1}^{(j)}) p(\mathbf{s}_k|\mathbf{s}_{k-1}^{(j)}).$$

Thus,

$$w_k^{(j)} \propto w_{k-1}^{(j)} p(\mathbf{z}_k|\mathbf{y}_k^{(j)}).$$

However, in this problem, the mobile state $\mathbf{x}_k$ and the sight condition state $\mathbf{s}_k$ constitute a high dimensional state space (Note: vector $\mathbf{s}_k$ has M independent components, totally 2^M states of sight conditions). Thus, to obtain an accurate estimation in such space, a large number of particles should be used, which prohibitively increases computational complexity. Additionally, in ranged-based outdoor positioning, where the covariance of the measurement noise in both LOS and NLOS conditions are much larger than that of the state noise, the overlapping region between the transition prior and the likelihood is relatively small. Without introducing the current step of measurements, the transition prior, used as the proposal in standard particle filtering, cannot sample from the interest region effectively, and this will cause the "particle impoverishment" problem after several iterations. Moreover, the standard particle filtering does not estimate the velocity effectively, because the weight only

reflects the similarity between the position component $\begin{bmatrix} x_k^{(j)} \\ y_k^{(j)} \end{bmatrix}$ of $\mathbf{x}_k^{(j)}$ and the actual position.

To reduce the dimension of the variable directly inferred by particle filtering, RBPF is proposed to decompose the state space into two parts, with one part being estimated by particle filtering while the other part being analytically calculated [25, 26]. As a result, the variance of the estimates can be reduced compared with the standard particle filtering [27]. RBPF has been previously investigated in mobile tracking in [28, 29], in which the mobile positions and command process are estimated with a particle filter, and the speeds and accelerations with a Kalman filter. However, the method could not directly be used in the problem of our concern, because of the hidden variable $s_{i,k}$ with different states that corrupt the measurement data in the observation model. Also the sight conditions $s_{i,k}$ between MS and different BS are assumed independent, which makes the problem more complicated.

Factorize the posterior $p(\mathbf{x}_k, \mathbf{s}_k|\mathbf{z}_{1:k})$ according to Bayes' rule:

$$p(\mathbf{x}_k, \mathbf{s}_k|\mathbf{z}_{1:k}) = p(\mathbf{x}_k|\mathbf{s}_k, \mathbf{z}_{1:k})p(\mathbf{s}_k|\mathbf{z}_{1:k}). \tag{14}$$

If the posterior density of $p(\mathbf{s}_k|\mathbf{z}_{1:k})$ could be represented by a set of weighted samples $\{\mathbf{s}_k^{(j)}, w_k^{(j)}\}_{j=1}^N$, i.e.,

$$p(\mathbf{s}_k|\mathbf{z}_{1:k}) \approx \sum_{j=1}^{N} w_k^{(j)} \delta(\mathbf{s}_k - \mathbf{s}_k^{(j)}), \tag{15}$$

Then, the marginal density $p(\mathbf{x}_k|\mathbf{z}_{1:k})$ can be approximately expressed by a mixture of densities:

$$\begin{aligned} p(\mathbf{x}_k|\mathbf{z}_{1:k}) &\approx \sum_{j=1}^{N} w_k^{(j)} p(\mathbf{x}_k|\mathbf{s}_k, \mathbf{z}_{1:k}) \delta(\mathbf{s}_k - \mathbf{s}_k^{(j)}) \\ &= \sum_{j=1}^{N} w_k^{(j)} p(\mathbf{x}_k|\mathbf{s}_k^{(j)}, \mathbf{z}_{1:k}), \end{aligned} \tag{16}$$

where the mixture component $p(\mathbf{x}_k|\mathbf{s}_k^{(j)}, \mathbf{z}_{1:k})$ approximately conforms to Gaussian distribution $\mathrm{N}(\hat{\mathbf{x}}_k^{(j)}, \hat{\mathrm{P}}_k^{(j)})$, which can be calculated by decentralized EKF, an extension to decentralized KF [30]:

$$\hat{\mathbf{x}}_k^{(j)} = \hat{\mathbf{x}}_{k|k-1}^{(j)} + \sum_{j=1}^{M} \mathrm{K}_{i,k}^{(j)} (z_{i,k} - \hat{z}_{i,k|k-1}^{(j)}) \tag{17}$$

$$\hat{\mathrm{P}}_k^{(j)} = \left[(\hat{\mathrm{P}}_{k|k-1}^{(j)})^{-1} + \sum_{i=1}^{M} (\mathrm{H}_{i,k}^{(j)})^T \mathrm{R}(s_{i,k}^{(j)})^{-1} \mathrm{H}_{i,k}^{(j)} \right]^{-1} \tag{18}$$

where $\hat{\mathbf{x}}_{k|k-1}^{(j)}$ is the predicted mean of $\mathbf{x}_{k-1}^{(j)}$:

$$\hat{\mathbf{x}}_{k|k-1}^{(j)} = \Phi \hat{\mathbf{x}}_{k-1}^{(j)} \tag{19}$$

and $\hat{\mathrm{P}}_{k|k-1}^{(j)}$ is the corresponding predicted covariance:

$$\hat{\mathrm{P}}_{k|k-1}^{(j)} = \Phi_{k-1} \hat{\mathrm{P}}_{k-1}^{(j)} \Phi_{k-1}^{T} + \mathrm{Q} \tag{20}$$

The predicted mean of measurement $\hat{z}_{i,k|k-1}^{(j)}$ is

$$\hat{z}_{i,k|k-1}^{(j)} = h_i(\hat{\mathbf{x}}_{k|k-1}^{(j)}) + m(s_{i,k}^{(j)}) \tag{21}$$

The Kalman gain is

$$\mathrm{K}_{i,k}^{(j)} = \hat{\mathrm{P}}_{i,k}^{(j)} (\mathrm{H}_{i,k}^{(j)})^{T} \mathrm{R}(s_{i,k}^{(j)})^{-1} \tag{22}$$

and $\mathrm{H}_{i,k}^{(j)} = \frac{\partial h_i}{\partial \mathbf{x}}|_{\mathbf{x}=\hat{\mathbf{x}}_{k|k-1}^{(j)}}$.

To sample $\mathbf{s}_k^{(j)}$ from $p(\mathbf{s}_k|\mathbf{z}_{1:k})$, the optimal trial distribution could minimize the variance of the importance weights [27]. Conditioned upon $\mathbf{s}_{k-1}^{(j)}, \mathbf{x}_{k-1}^{(j)}$ and $\mathbf{z}_k$, the optimal trial distribution is:

$$\begin{aligned} q(\mathbf{s}_k|\mathbf{s}_{k-1}^{(j)}, \mathbf{x}_{k-1}^{(j)}, \mathbf{z}_k)_{\text{opt}} &= \mathrm{P}(\mathbf{s}_k|\mathbf{s}_{k-1}^{(j)}, \mathbf{x}_{k-1}^{(j)}, \mathbf{z}_k) \\ &= \frac{p(\mathbf{z}_k|\mathbf{s}_k, \mathbf{x}_{k-1}^{(j)}) \mathrm{P}(\mathbf{s}_k|\mathbf{s}_{k-1}^{j})}{p(\mathbf{z}_k|\mathbf{s}_{k-1}^{(j)}, \mathbf{x}_{k-1}^{(j)})} \end{aligned} \tag{23}$$

where $p(\mathbf{z}_k|\mathbf{s}_k, \mathbf{x}_{k-1}^{(j)})$ can be further approximated as:

$$\begin{aligned} p(\mathbf{z}_k|\mathbf{s}_k, \mathbf{x}_{k-1}^{(j)}) &= \int p(\mathbf{z}_k|\mathbf{s}_k, \mathbf{x}_k) p(\mathbf{x}_k|\mathbf{x}_{k-1}^{(j)}) \mathrm{d}\mathbf{x}_k \\ &\approx \int p(\mathbf{z}_k|\mathbf{s}_k, \mathbf{x}_k) \delta(\mathbf{x}_k - \hat{\mathbf{x}}_{k|k-1}^{(j)}) \mathrm{d}\mathbf{x}_k \\ &= p(\mathbf{z}_k|\mathbf{s}_k, \hat{\mathbf{x}}_{k|k-1}^{(j)}) \end{aligned} \tag{24}$$

Based on the independent transition of the M sight conditions (11), the trial distribution (23) can be further expressed as

$$q(\mathbf{s}_k|\mathbf{s}_{k-1}^{(j)}, \mathbf{x}_{k-1}^{(j)}, \mathbf{z}_k) = \frac{\prod_{i=1}^{M} p(z_{i,k}|\hat{\mathbf{x}}_{k|k-1}^{(j)}, s_{i,k}) \mathrm{P}(s_{i,k}|s_{i,k-1}^{(j)})}{p(\mathbf{z}_k|\mathbf{s}_{k-1}^{(j)}, \mathbf{x}_{k-1}^{(j)})}, \tag{25}$$

The likelihood $p(z_{i,k}|\hat{\mathbf{x}}_{k|k-1}^{(j)}, s_{i,k}^{(j)})$ conforms approximately to a Gaussian distribution with mean $\hat{z}_{i,k|k-1}^{(j)}$ (21) and covariance:

$$\hat{\Sigma}_{i,k|k-1}^{(j)} = \mathrm{H}_{i,k}^{(j)} \hat{\mathrm{P}}_{k|k-1}^{(j)} (\mathrm{H}_{i,k}^{(j)})^{T} + \mathrm{R}(s_{i,k}^{(j)}). \tag{26}$$

The corresponding importance weight can be calculated as

$$\begin{aligned} w_k^{(j)} &\propto w_{k-1}^{(j)} p(\mathbf{z}_k|\mathbf{s}_{k-1}^{(j)}, \mathbf{x}_{k-1}^{(j)}) \\ &= w_{k-1}^{(j)} \sum_{\mathbf{s}_k} \left[p(\mathbf{z}_k|\mathbf{s}_k, \mathbf{x}_{k-1}^{(j)}) \mathrm{P}(\mathbf{s}_k|\mathbf{s}_{k-1}^{(j)}) \right] \\ &= w_{k-1}^{(j)} \sum_{\mathbf{s}_k} \left[\prod_{i=1}^{M} p(z_{i,k}|\mathbf{x}_{k|k-1}^{(j)}, s_{i,k}) \mathrm{P}(s_{i,k}|s_{i,k-1}^{(j)}) \right]. \end{aligned} \tag{27}$$

From (27), the importance weight $w_k^{(j)}$ only depends on the current measurement $\mathbf{z}_k$ and the particles of t_{k-1}, i.e. $\{\hat{\mathbf{x}}_{k-1}^{(j)}, \hat{\mathrm{P}}_{k-1}^{(j)}, \mathbf{s}_{k-1}^{(j)}\}_{j=1}^{N}$, while $\mathbf{s}_k$ is marginalized out. Thus, to improve the sample effectiveness, the particles of t_{k-1} could be selected (resampled) based on current measurement $\mathbf{z}_k$, and the fittest particles could be allowed to propagate. Then, new particles could be sampled from $\mathbf{s}_k$ based on $\mathbf{s}_{k-1}^{(j)}, \mathbf{x}_{k-1}^{(j)}$ and $\mathbf{z}_k$ according to (25).

Algorithm 1 summarizes the whole scheme.

Algorithm 1: Improved RBPF method

for $k = 1, 2, \ldots$ **do**
  for $j = 1, 2, \ldots, N$ **do**
    Compute predicted mean $\hat{\mathbf{x}}_{k|k-1}^{(j)}$ and covariance $\hat{\mathrm{P}}_{k|k-1}^{(j)}$ using (19),(20) and new weight $w_k^{(j)}$ using (27).
  end for
  Resample particles $\{w_k^{(j)}, \mathbf{s}_{k-1}^{(j)}, \hat{\mathbf{x}}_{k|k-1}^{(j)}, \hat{\mathrm{P}}_{k|k-1}^{(j)}\}_{j=1}^{N}$ using new weights $w_k^{(j)}$ to obtain
  $\{w_k^{(l)}, \mathbf{s}_{k-1}^{(l)}, \hat{\mathbf{x}}_{k|k-1}^{(l)}, \hat{\mathrm{P}}_{k|k-1}^{(l)}\}_{l=1}^{N}$, where $w_k^{(l)} = \frac{1}{N}$.
  for $l = 1, 2, \ldots, N$ **do**
1. Sample $\mathbf{s}_k^{(l)} \sim \mathrm{P}(\mathbf{s}_k|\mathbf{s}_{k-1}^{(l)}, \mathbf{z}_k)$ according to (25).
2. Update using prior particles $\{\mathbf{s}_{k-1}^{(l)}, \hat{\mathbf{x}}_{k|k-1}^{(l)}, \hat{\mathrm{P}}_{k|k-1}^{(l)}\}_{l=1}^{N}$ and decentralized EKF according to (17)-(22) to obtain $\{\mathbf{s}_k^{(l)}, \hat{\mathbf{x}}_k^{(l)}, \hat{\mathrm{P}}_k^{(l)}\}_{l=1}^{N}$.
  end for
end for

The advantage of the RBPF method is that by introducing the factorization of the posterior $p(\mathbf{x}_k, \mathbf{s}_k|\mathbf{z}_{1:k})$, we could use PF to estimate the marginal posterior $p(\mathbf{s}_k|\mathbf{z}_{1:k})$ first, then use decentralized EKF to analytically compute the mean and covariance of the mobile state. As a result of the marginalization, the covariance of the estimate can be reduced compared with the standard PF.

In particle filtering, in order to achieve the minimum weight conditional variance of importance weights, we choose the optimal trial distribution. According to the description of Algorithm 1, the resampling step is implemented before sampling step, and the fittest particles are chosen to propagate, thus

the particle effectiveness is improved. In contrast with the standard particle filtering in RBPF[31], the proposed method is called an improved RBPF (I-RBPF).

4 Lower bound of performance

An error lower bound gives an indication of performance limitations. In time-invariant statistical models, Cramé-Rao bound (CRB) is commonly used. In the time-varying systems context we deal with here, a CRB for random parameters is referred to as posterior CRLB (PCRLB) [32, p. 66-86]. The PCRLB for the joint estimation of $\mathbf{y}_k \triangleq \begin{bmatrix} \mathbf{x}_k \\ \mathbf{s}_k \end{bmatrix}$ is bounded by I_k^{-1}, where I_k is the posterior FIM:

$$\mathrm{I}_k = \mathrm{E}\{-\Delta_{\mathbf{y}_k}^{\mathbf{y}_k} \log p(\mathbf{y}_k, \mathbf{z}_k)\}, \tag{28}$$

$\Delta_{\Theta}^{\Psi} = \nabla_{\Theta} \nabla_{\Psi}^T$, ∇ is first order derivative operator.

It is not possible to compute the close-form solution because it requires that all associated probability density functions must be continuously differentiable [24, Chapter 4.4]. However, for a discrete variant $\mathbf{s}_k$, the differentiation of $p(\mathbf{s}_{k+1}|\mathbf{s}_k)$ does not exit. As an alternative, we here to compute a kind of PCRLB under the assumption that LOS and NLOS transition history is known, which avoids the false detection of sight condition.

By assuming the sight condition $\mathbf{s}_k$ is known, only $\mathbf{x}_k$ is to be estimated. Let $\hat{\mathbf{x}}_k$ be an estimator of $\mathbf{x}_k$ based on the measurements $\mathbf{z}_{1:k}$. Then, the estimate covariance P_k is bounded by the PCRLB J_k^{-1}

$$\begin{aligned} \mathrm{P}_k &= \mathrm{E}\{[\hat{\mathbf{x}}_k - \mathbf{x}_k][\hat{\mathbf{x}}_k - \mathbf{x}_k]^T\} \geq \mathrm{J}_k^{-1} \\ \mathrm{J}_k &= \mathrm{E}\{-\Delta_{\mathbf{x}_k}^{\mathbf{x}_k} \log p(\mathbf{x}_k, \mathbf{z}_k)\} \end{aligned} \tag{29}$$

Tichavsky et al [33] show that the FIM J_k can be recursively calculated as

$$\mathrm{J}_{k+1} = \mathrm{D}_k^{22} - \mathrm{D}_k^{21}(\mathrm{J}_k + \mathrm{D}_k^{11})\mathrm{D}_k^{12}, \tag{30}$$

where

$$\mathrm{D}_k^{11} = \mathrm{E}\left\{-\Delta_{\mathbf{x}_k}^{\mathbf{x}_k} \log f(\mathbf{x}_{k+1}|\mathbf{x}_k)\right\} \overset{(1)}{=} \Phi_k^T {\mathrm{Q}_k}^{-1} \Phi_k \tag{31a}$$

$$\mathrm{D}_k^{12} = \left[\mathrm{D}_k^{21}\right]^T = \mathrm{E}\left\{\Delta_{\mathbf{x}_k}^{\mathbf{x}_{k+1}} \log f(\mathbf{x}_{k+1}|\mathbf{x}_k)\right\} \overset{(1)}{=} -\Phi_k^T {\mathrm{Q}_k}^{-1} \tag{31b}$$

$$\mathrm{D}_k^{22} = \mathrm{E}\left\{-\Delta_{\mathbf{x}_k}^{\mathbf{x}_{k+1}} \log f(\mathbf{x}_{k+1}|\mathbf{x}_k)\right\} + \underbrace{\mathrm{E}\left\{\Delta_{\mathbf{x}_{k+1}}^{\mathbf{x}_{k+1}} \log f(\mathbf{z}_{k+1}|\mathbf{x}_{k+1})\right\}}_{\Psi_k} \overset{(1)}{=} \mathrm{Q}_k^{-1} + \Psi_k \tag{31c}$$

and the recursion (30) is initialized with

$$\mathrm{J}_0 = \mathrm{E}\{-\Delta_{\mathbf{x}_0}^{\mathbf{x}_0} \log p(\mathbf{x}_0)\}. \tag{32}$$

Apply the inverse matrix lemma:

$$\mathrm{J}_{k+1} = (\mathrm{Q}_k + \Phi_k \mathrm{J}_k^{-1} \Phi_k^T)^{-1} + \Psi_k \tag{33}$$

Ψ_k relates to nonlinear measurement equation:

$$\begin{aligned}
\Psi_k &= \frac{1}{2}\mathrm{E}\left\{\Delta_{\mathbf{x}_{k+1}}^{\mathbf{x}_{k+1}} \left[\mathbf{z}_{k+1} - \mathbf{h}(\mathbf{x}_{k+1}) - m(\mathbf{s}_{k+1})\right]^T \Sigma_{k+1}^{-1} \left[\mathbf{z}_{k+1} - \mathbf{h}(\mathbf{x}_{k+1}) - m(\mathbf{s}_{k+1})\right]\right\} \\
&\approx \mathrm{E}_{p(\mathbf{x}_{k+1}, \mathbf{z}_{k+1})} \left\{ \mathrm{H}(\mathbf{x}_{k+1})^T \Sigma_{k+1}^{-1} \mathrm{H}(\mathbf{x}_{k+1}) \right\} \\
&= \mathrm{E}_{\mathbf{z}_{k+1}} \underbrace{\mathrm{E}_{p(\mathbf{x}_{k+1}|\mathbf{z}_{k+1})} \left\{ \mathrm{H}(\mathbf{x}_{k+1})^T \Sigma_{k+1}^{-1} \mathrm{H}(\mathbf{x}_{k+1}) \right\}}_{\Lambda_k}
\end{aligned} \tag{34}$$

where $\mathrm{H}(\mathbf{x}_{k+1}) = [\mathrm{H}_1(\mathbf{x}_{k+1}), ..., \mathrm{H}_M(\mathbf{x}_{k+1})]^T$ and $\mathrm{H}_i(\mathbf{x}_{k+1}) = \frac{\partial h_i(\mathbf{x})}{\partial \mathbf{x}}|_{\mathbf{x}=\mathbf{x}_{k+1}}$.

By assuming the sight conditions known, $p(\mathbf{x}_{k+1}|\mathbf{z}_{k+1})$ is approximately conformed to Gaussian distribution, which can be computed by the decentralized EKF method:

$$\hat{\mathbf{x}}_{k+1} = \hat{\mathbf{x}}_{k+1|k} + \sum_{i=1}^{M} \mathrm{K}_{i,k+1}(z_{i,k+1} - \hat{z}_{i,k+1|k}) \tag{35a}$$

$$\hat{\mathrm{P}}_{k+1} = [\hat{\mathrm{P}}_{k+1|k}^{-1} + \sum_{i=1}^{M} (\mathrm{H}_i(\hat{\mathbf{x}}_{k+1|k}))^T \mathrm{R}(s_{i,k+1})^{-1} \mathrm{H}_i(\hat{\mathbf{x}}_{k+1|k})]^{-1} \tag{35b}$$

$$\hat{\mathrm{P}}_{i,k+1} = \left[\hat{\mathrm{P}}_{k+1|k}^{-1} + (\mathrm{H}_i(\hat{\mathbf{x}}_{k+1|k}))^T \mathrm{R}(s_{i,k+1})^{-1} \mathrm{H}_i(\hat{\mathbf{x}}_{k+1|k})\right]^{-1} \tag{35c}$$

$$\mathrm{K}_{i,k+1} = \hat{\mathrm{P}}_{i,k+1} (\mathrm{H}_i(\hat{\mathbf{x}}_{k+1|k}))^T \mathrm{R}(s_{i,k+1})^{-1} \tag{35d}$$

$$\hat{z}_{i,k+1|k} = h_i(\hat{\mathbf{x}}_{k+1|k}) + m(s_{i,k+1}) \tag{35e}$$

Assume a n_x dimension state variable $\mathbf{x}_{k+1} \sim \mathrm{N}(\hat{\mathbf{x}}_{k+1}, \hat{\mathrm{P}}_{k+1})$, a set of $2n_x+1$ sigma points $SS_{k+1}^{(j)} = \left\{W_{k+1}^{(j)}, \mathbf{x}_{k+1}^{(j)}\right\}$ can be deterministically sampled from this multivariate Gaussian distribution (Table 1). Parameter $\kappa > 0$ is a scaling parameter.

Table 1 Symmetric Sigma Points Set of $\mathrm{N}\left(\hat{\mathbf{x}}_k, \hat{\mathrm{P}}_k\right)$

Index (j)	Weight ($W_{k+1}^{(j)}$)	Sigma point ($\mathbf{x}_{k+1}^{(j)}$)
0	$\frac{\kappa}{n_x+\kappa}$	$\hat{\mathbf{x}}_{k+1}$
$1, \ldots, n_x$	$\frac{1}{2(n_x+\kappa)}$	$\hat{\mathbf{x}}_{k+1} + \left(\sqrt{(n_x+\kappa)\hat{\mathrm{P}}_{k+1}}\right)_j$
$n_x+1, \ldots, 2n_x$	$\frac{1}{2(n_x+\kappa)}$	$\hat{\mathbf{x}}_{k+1} - \left(\sqrt{(n_x+\kappa)\hat{\mathrm{P}}_{k+1}}\right)_j$

Based on sigma points $SS_{k+1}^{(j)}$, the expectation Λ_k is:

$$\Lambda_k = \sum_{j=0}^{2n_x} \left[\mathrm{H}(\mathbf{x}_{k+1}^{(j)})^T \Sigma_{k+1}^{-1} \mathrm{H}(\mathbf{x}_{k+1}^{(j)}) \right] W_k^{(j)}. \tag{36}$$

To get Ψ_k, which is the expectation with respect to $p(\mathbf{z}_{k+1})$, we set up Monte Carlo simulation: according to one specific sight condition sequence $\mathbf{s}_{1:k}$, L different trajectories could be generated with different measurements: $\{\mathbf{z}_{1:k}^1, \cdots, \mathbf{z}_{1:k}^L\}$. For each $\{\mathbf{z}_{1:k}^l\}$, $(l \in 1:L)$, Λ_k^l can be computed according to (36). Then,

$$\Psi_k = \frac{1}{L} \sum_{l=1}^{L} \Lambda_k^l \tag{37}$$

To get a general PCRLB which does not rely on one specific known sight condition, Monte Carlo simulations could be set with different sight conditions: $\{\mathbf{s}_{1:k}^1, \cdots, \mathbf{s}_{1:k}^{\mathrm{MC}}\}$. By assuming each of the sight condition $\{\mathbf{s}_{1:k}^{\mathrm{mc}}\}$ is known, the corresponding specific PCRLB is then computed as:

$$\mathrm{PCRLB}^{\mathrm{mc}}(\mathbf{x}_k) = [\mathrm{J}_k^{\mathrm{mc}}]^{-1} \tag{38}$$

Then the general PCRLB is defined as the expected value of specific CRLB:

$$\mathrm{PCRLB}(\mathbf{x}_k) = \mathrm{E}\left\{ \mathrm{PCRLB}^{\mathrm{mc}}(\mathbf{x}_k) \right\} = \frac{1}{\mathrm{MC}} \sum_{\mathrm{mc}=1}^{\mathrm{MC}} [\mathrm{J}_k^{\mathrm{mc}}]^{-1} \tag{39}$$

Algorithm 2 gives a detailed scheme to compute PCRLB.

Algorithm 2: PCRLB computation

for mc $= 1, 2, \ldots$ MC **do**
  for $k = 1, 2, \ldots$ **do**
    for $l = 1, 2, \ldots L$ **do**
1. Update the $\{\hat{\mathbf{x}}_{k+1}^{\mathrm{mc},l}, \hat{\mathrm{P}}_{k+1}^{\mathrm{mc},l}\}$ according to (35a)-(35b) with one specific sight condition $\{\mathbf{s}_{1:k}^{\mathrm{mc}}\}$ known.
2. Deterministically choose a set of $2n_x+1$ sigma points $SS_{k+1}^{(j),\mathrm{mc},l} = \left\{ W_{k+1}^{(j),\mathrm{mc},l}, \mathbf{x}_{k+1}^{(j),\mathrm{mc},l} \right\}$ according to Table 1.
3. Compute $\Lambda_k^{22,b,\mathrm{mc}}$ according to (36).

    end for
    Compute Ψ_k^{mc} according to (37).
    Update $\mathrm{J}_{k+1}^{\mathrm{mc}}$ according to (33).
    Compute $\mathrm{PCRLB}^{\mathrm{mc}}(\mathbf{x}_k)$ according to (38)
  end for
end for
Compute $\mathrm{PCRLB}(\mathbf{x}_k)$ according to (39).

Symmetric sigma set and unscented transformation method computes mean and covariance to second order accuracy [34]. Thus, based on the analytical estimate of the mobile state, and the deterministical sampling method using sigma set and unscented transformation, the PCRLB can be effectively calculated. This bound is not achieved by any filter, because it assumes the knowledge of the sight condition is known. In other words, the detection probability of the sight condition is correctly detected, which is not possible for a practical algorithm. Nevertheless, the bound could also provide useful information in predicting the performance for various sampling intervals and sensor accuracy [24, p. 80].

5 Numerical results and performance evaluation

In the simulation, MS is assumed to be able to receive the signals from three BS all the time. The coordinates of BS are [-3.0 km, -1.0 km], [-3.0 km, 5.0 km], [5.0 km, -1.0 km]. The mobile trajectories are generated according to the mobility model described in Section 2., in which the initial position of the MS is set to [-1.5 km, 1.5 km], and the initial velocity is set as [20 m/s, 0 m/s]. The random acceleration variances σ_x^2, σ_y^2 are both chosen to 0.5 $(\mathrm{m/s^2})^2$. The simulated trajectory has $L = 1600$ time samples, and the sample interval $\Delta t = 0.2$ s. The simulated measurement data are generated by adding the measurement noise and the NLOS noise to the true distance from MS to each BS. The measurement noise is assumed to be a white random variable with zero mean and standard deviation $\sigma_m = 150$ m, whereas the NLOS measurement noise is also assumed to be a white random variable with positive mean $\mu_{\mathrm{NLOS}} = 513$ m, and standard deviation $\sigma_{\mathrm{NLOS}} = 409$ m [13]. The sight condition between the MS and each BS is changed every 200 samples [14, 15, 18].

The performance of the IMM [15], the modified EKF banks [18] and the I-RBPF method are compared. Different number of particles are used in the I-RBPF method, denoted as I-RBPF(N) for brevity. The initial position is calculated by Chan's algorithm [35] using the first three range measurements. For vague prior of the mobile state, the initial velocity is set as [0 m/s, 0 m/s] and the covariance matrix $\mathrm{C}_{t0} = \begin{bmatrix} 150^2 \cdot \mathrm{I}_2 & 0 \\ 0 & 20^2 \cdot \mathrm{I}_2 \end{bmatrix}$ corresponding to a standard deviation of 150 m for the position and 20 m/s (72 km/h) for the velocity of each coordinate. The initial estimation of sight condition is set to $\mathrm{P}(s_{i,0} = 0) = \mathrm{P}(s_{i,0} = 1) = 0.5$, where $i = 1$, 2 and 3. All the simulation results are obtained based on $n_{\mathrm{mc}} = 50$ Monte Carlo realizations with the same parameters. The mobile location error is calculated with the elimination of the first 100 samples so as to ignore the large location error caused by the initial conditions. The evaluation index used in the evaluation are defined as: (1) Root Square Error (RSE):

$$\mathrm{RSE} \triangleq \sqrt{(\hat{x}_k - x_k)^2 + (\hat{y}_k - y_k)^2} \tag{40}$$

(2) Root Mean Square Error(RMSE) at time k :

$$\mathrm{RMSE}_k \triangleq \sqrt{\frac{1}{n_{\mathrm{mc}}} \sum_{m=1}^{n_{\mathrm{mc}}} [(\hat{x}_{k,m} - x_k)^2 + (\hat{y}_{k,m} - y_k)^2]} \tag{41}$$

(3) Average RMSE:

$$\text{Average RMSE} \triangleq \frac{1}{L} \sum\nolimits_{k=1}^{L} \mathrm{RMSE}_k \tag{42}$$

5.1 Performance comparison

Fig. 2 shows the position RMSE versus time and Fig. 3 shows the CDF of RSE. The prior transition probability of LOS/NLOS is set as $p_0 = p_1 = 0.85$. From Fig. 2 and 3, the I-RBPF(100) has slightly better performance than I-RBPF(10), while both I-RBPF(100) and I-RBPF(10) can track more accurately than the IMM and modified EKF method. The CDF and RMSE of PCRLB are also given in Fig. 2 and 3. The PCRLB is derived under 50 randomly generated sight conditions. For each sight condition sequence, 50 different trajectories are generated. From Fig. 3 , although the bound is based on the sight conditions known, the I-RBPF method approaches to the bound.

Fig. 4 gives the estimated and actual trajectories in a single realization. For the safe of the clarity in the figure, the trajectory of I-RBPF(10) is omitted, as it is indistinguishable form I-RBPF(100).

Table 2 shows the impact of different prior transition probabilities on the algorithms. Since the transition matrix assumes symmetric in the simulations, the values are studied from 0.55 to 0.997. The sight condition of each BS is changed for every 200 samples, which corresponds to a prior transition probability $p_0 = p_1 = 0.995$ [15]. From Table 2, the larger setting errors in the prior transition probability lead to larger tracking errors in all the algorithms. However, I-RBPF can track more effectively than the others, which suggests that I-RBPF can estimate the posterior distribution more correctly despite of prior setting errors. The improvement may come from its optimal sampling distribution and effective particle selecting mechanisms. The prior transition probabilities of sight conditions did not have obvious influence to the PCRLB, because the sight conditions are assumed known.

5.2 Complexity comparison

Table 3 compares the relative complexity and precision of the algorithms with the prior transition probability $p_0 = p_1 = 0.85$. It is clear that with the increase of the particle numbers, the computing time of the I-RBPF increases

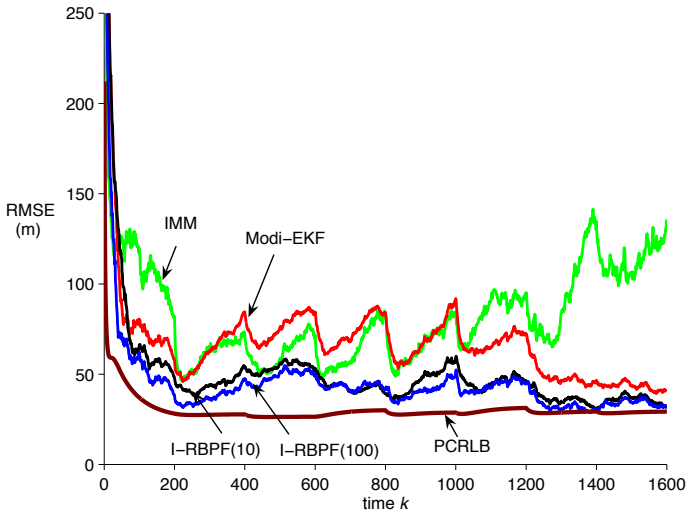

Fig. 2 Position RMSE vs. Time instant ($p_0 = p_1 = 0.85$)

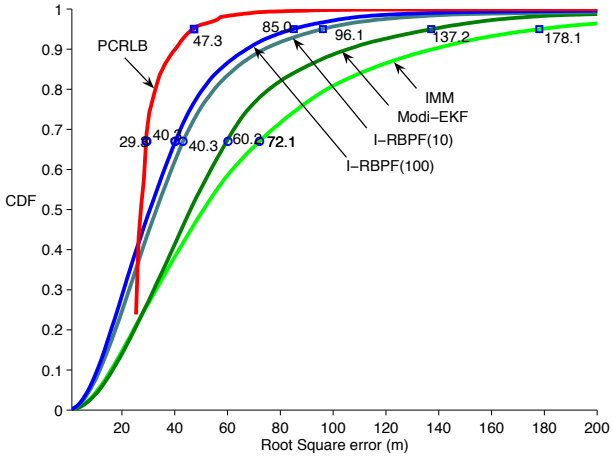

Fig. 3 CDF of RSE ($p_0 = p_1 = 0.85$)

proportionally. Accordingly, the precision also increases. But the improvement is slight when the number is larger than 10. Also, there is almost no precision difference when using 100 and 1000 particles. Thus, it can be concluded that I-RBPF(10) achieves a good tradeoff between complexity and precision.

To sum up, in this section, we compare the performance of three methods and also with PCRLB in LOS/NLOS transition conditions. Simulation tests show that the I-RBPF method has better performance than the other two. Increasing the number of the particles will improve the estimation accuracy of I-RBPF. Numerical results also suggests that the error performances of I-RBPF both with 10 particles and 100 particles approaches to PCRLB when

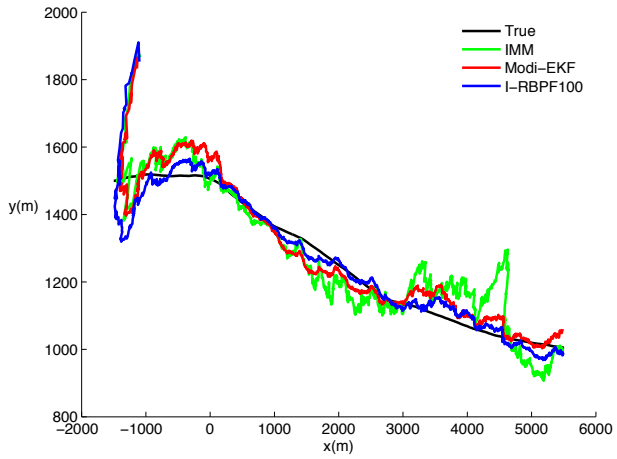

Fig. 4 The estimated and actual trajectories of the MS in a single realization

Table 2 Average RMSE vs. Transition Probability of Sight Condition

	0.55	0.65	0.75	0.85	0.95	0.995	0.997
IMM	201.5	158.5	113.8	83.2	57.6	52.1	52.8
Modi-EKF	115.2	108.0	81.9	68.6	53.7	48.6	46.9
I-RBPF(10)	109.6	92.4	73.3	50.8	48.6	45.5	44.1
I-RBPF(100)	109.6	92.3	69.4	45.2	42.5	40.2	41.3
PCRLB	38.2	38.5	37.2	36.2	37.1	36.1	36.2

Table 3 Complexity vs. Precision

	IMM	Modi-EKF	I-RBPF						
			1	4	10	30	50	100	1000
Complexity	1	1.6	0.7	2	4.9	14.1	23.3	46.3	462.3
Precision	1	1.21	1.06	1.28	1.64	1.71	1.78	1.84	1.84

Complexity is based on the CPU running time of the algorithms and the value is proportion to that of IMM method. The precision is the reciprocal of the average RMSE that each algorithm achieves, and also the precision of IMM is normalized.

the sight conditions can be correctly detected. Complexity analysis suggests that the I-RBPF method with 10 particles achieves a good tradeoff between complexity and precision.

6 Conclusion and further work

An improved RBPF method has been proposed for mobile localization in mixed LOS and NLOS conditions. The algorithm estimates the sight condition state using particle filtering, in which particles are sampled by the optimal trial distribution and selected by one-step backward prediction. By applying decentralized EKF method, the mobile state could then be analytically computed.

Simulation shows that compared with current methods, the algorithm achieves more accurate estimation and is less influenced by setting errors of transition probability. Moreover, the theoretical error lower bound is also studied, which assumes that the LOS and NLOS transition history is known. Although the bound is over optimistic that could not be achieved by any practical method, simulation results show that the error performances of I-RBPF approaches to the bound when the sight conditions can be correctly detected.

Further work will relax the assumption that the sight transition sequence is known and use the Markov chain model of the sight condition to calculate the theoretical bound.

References

1. M. I. Silventoinen and T. Rantalainen, "Mobile station emergency locating in GSM," in *Proceedings of IEEE International Conference on Personal Wireless Communications*, Dallas, Texas, June 1996, pp. 232–238.
2. J. Borras, P. Hatrack, and N. B. Mandayam, "Decision theoretic framework for NLOS identification," in *Proceedings of IEEE Vehicular Technology Conference*, Ottawa, Canada, May 1998, pp. 731–734.
3. L. Xiong, "A selective model to suppress NLOS signals in angle-of-arrival (AOA)," in *Proceedings of IEEE International Symposium on Personal, Indoor and Mobile Radio Communications*, Boston, USA, 1998, pp. 1028–1031.
4. J. Riba and A. Urruela, "A non-line-of-sight mitigation technique based on ML-detection," in *Proceedings of IEEE International Conference on Acoustics, Speech, and Signal Processing*, vol. 2, Montreal QC, Canada, May 2004, pp. 153–156.
5. Y. T. Chan, W. Y. Tsui, H. C. So, and P. C. Ching, "Time-of-arrival based localization under NLOS conditions," *IEEE Transactions on Vehicular Technology*, vol. 55, no. 1, pp. 17–24, 2006.
6. P. C. Chen, "A non-line-of-sight error mitigation algorithm in location estimation," in *Proceedingsof IEEE Wireless Communications Networking Conference*, September 1999, pp. 316–320.
7. L. Cong and W. Zhang, "Non-line-of-sight error mitigation in TDOA mobile location," in *Proceedings of IEEE GLOBECOM*, vol. 1, San Antonio, Texas, Dec 2001, pp. 680–684.
8. N. Khajehnouri and A. H. Sayed, "A non-line-of-sight equalization scheme for wireless cellular location," in *Proceedings of IEEE Conference on Acoustics, Speech, and Signal Processing*, vol. 6, April 2003, pp. 549–552.
9. S. Al-Jazzar, J. J. Caffery, and H. R. You, "A scattering model based approach to NLOS mitigation in TOA location systems," in *Proceedings of IEEE Vehicular Technology Conference*, vol. 2, Birmingham, UK, May 2002, pp. 861–865.

10. S. Al-Jazzar and J. J. Caffery, "ML and Bayesian TOA location estimators for NLOS environments," in *Proceedings of IEEE Vehicular Technology Conference*, vol. 2, Birmingham, UK, May 2002, pp. 1178–1181.
11. Y. Qi, H. Kobayashi, and H. Suda, "Analysis of wireless geolocation in a non-line-of-sight environment," *IEEE Transactions on Wireless Communications*, vol. 5, no. 3, pp. 672–681, 2006.
12. H. Miao, K. Yu, and M. J. Juntti, "Positioning for NLOS propagation: algorithm derivation and Cramer-Rao bounds," *IEEE Transactions on Vehicular Technology*, vol. 56, no. 5, pp. 2568–2580, 2007.
13. M. P. Wylie and J. Holtzman, "The nonline of sight problem in mobile location estimation," in *Proceedings of IEEE International Conference on Universal Personal Communications*, vol. 2, 1996, pp. 827–831.
14. B. L. Le, K. Ahmed, and H. Tsuji, "Mobile location estimatior with NLOS mitigation using Kalman filtering," in *IEEE Wireless Communications and Networking Conference*, vol. 3, New Orleans, USA, 2003, pp. 1969–1973.
15. B.-S. Chen, C.-Y. Yang, F.-K. Liao, and J.-F. Liao, "Mobile location estimator in a rough wireless environment using extended Kalman-based IMM and data fusion," *IEEE Transactions on Vehicular Technology*, vol. 58, no. 3, pp. 1157–1169, March 2009.
16. C. Morelli, M. Nicoli, V. Rampa, and U. Spagnolini, "Hidden Markov models for radio localization in mixed LOS/NLOS conditions," *IEEE Transactions on Signal Processing*, vol. 55, no. 4, pp. 1525–1542, 2007.
17. M. Nicoli, C. Morelli, and V. Rampa, "A jump Markov particle filter for localization of moving terminals in multipath indoor scenarios," *IEEE Transactions on Signal Processing*, vol. 56, no. 8, pp. 3801–3809, Aug. 2008.
18. L. Chen and L. Wu, "Mobile positioning in mixed LOS/NLOS conditions using modified EKF banks and data fusion method," *IEICE Transactions on Communications*, vol. EB92, no. 4, pp. 1318–1325, April 2009.
19. "Revision of the commissions rules to insure compatibility with enhanced 911 emergency calling systems," Federal Communication Commission (FCC), Washington, DC, Tech. Rep. RM-8134, 1996. [Online]. Available: http://www.fcc.gov
20. Y. Bar-Shalom, R. X. Li, and T. Kirubarajan, *Estimation with Applications to Tracking and Navigation, Theory Algorithms and Software.* John Wiley & Sons, 2001.
21. L. Chen and L. Wu, "Mobile localization with NLOS mitigation using improved Rao-Blackwellized particle filtering algorithm," in *Proceedings of 13th IEEE International Symposium on Consumer Electronics*, Kyoto, Japan, May 2009.
22. L. Chen, L. Wu, and R. Piché, "Posterior Cramer-Rao bounds for mobile tracking in mixed LOS/NLOS conditions," in *Proceedings of 17th European Signal Processing Conference*, Glasgow, Scotland, August 2009, pp. 90–94.

23. A. F. Molisch, H. Asplund, and R. Heddergott, "The COST259 directional channel model - Part I: overview and methodology," *IEEE Transactions on Wireless Communications*, vol. 5, no. 12, pp. 3421–3433, 2006.
24. B. Ristic, S. Arulampalam, and N. Gordon, *Beyond the Kalman Filter, Particle Filters for Tracking Applications*. Boston, London: Artech House, 2004.
25. A. Doucet, N. de Freitas, K. Murphy, and S. Russell, "Rao-Blackwellized particle filtering for dynamic Bayesian networks," in *Proceedings of UAI2000*, 2000, pp. 176–183.
26. R. Chen and J. Liu, "Mixture Kalman filters," *Journal of the Royal Statistics Society, series B*, vol. 62, pp. 493–508, 2000.
27. M. S. Arulampalam, S. Maskell, N. Gordon, and T. Clapp, "A tutorial on particle filters for online nonlinear/non-Gaussian Bayesian tracking," *IEEE Transactions on Signal Processing*, vol. 50, no. 2, pp. 174–188, 2002.
28. F. Gustafsson and F. Gunnarsson, "Mobile positioning using wireless networks: possibilities and fundamental limitations based on available wireless network measurements," *Signal Processing Magazine, IEEE*, vol. 22, no. 4, pp. 41–53, July 2005.
29. L. Mihaylova, D. Angelove, S. Honary, D. R. Bull, C. N. Canagarajah, and B. Ristic, "Mobility tracking in cellular networks using particle filtering," *IEEE Transactions on Wireless Communications*, vol. 6, no. 10, pp. 3589–3599, Oct. 2007.
30. H. Whyte, B. Y. Yao, and H. Hu, "Toward a fully decentralized architecture for multi-sensor data fusion," in *Proceedings of IEEE International Conference on Robotics and Automation*, vol. 2, New Jersey, USA, May 1990, pp. 1331–1336.
31. J. F. G. de Freitas, "Rao-Blackwellized particle filtering for fault diagnosis," in *Proceedings of Aerospace Conference*, vol. 4, 2002, pp. 1767–1772.
32. H. L. van Trees, *Detection, Estimation and Modulation Theory*. New York: Wiley, 1968, vol. I.
33. P. Tichavsky, C. H. Muravchik, and A. Nehorai, "Posterior Cramer-Rao bounds for discrete-time nonlinear filtering," *IEEE Transactions on Signal Processing*, vol. 46, no. 5, pp. 1386–1396, May 1998.
34. S. J. Julier and J. K. Uhlmann, "Unscented filtering and nonlinear estimation," *Proceedings of the IEEE*, vol. 92, no. 3, pp. 401–422, March 2004.
35. Y. T. Chan and K. C. Ho, "A simple and efficient estimator for hyperbolic location," *IEEE Transactions on Signal Processing*, vol. 42, no. 8, pp. 1905–1915, 1994.